한국소음진동공학회지 제 6 권 제 5 호, pp. 587~594, 1996.

〈Original Paper〉

Free Vibrations and Buckling Loads of Tapered Beam-Columns of Regular Polygon Cross-Section with Constant Volume

일정체적의 정다각형 단면을 갖는 변단면 보-기둥의 자유진동 및 좌굴하중

Byoung Koo Lee* and Jeong Man Mo**

이 병 구·모 정 만

(Received May 29, 1996 ; Accepted September 7, 1996)

Key Words : Buckling Load(좌굴하중), Constant Volume(일정체적), Free Vibration(자유진동), Regular Polygon Cross-Section(정다각형단면), Strongest Column(최강기둥), Tapered Beam-Column (변단면 보-기둥)

ABSTRACT

The differential equations governing both the free vibrations and buckling loads of tapered beam-columns of regular polygon cross-section with constant volume were derived and solved numerically. The parabolic and sinusoidal tapers were chosen as the variable depth of cross-section for the tapered beam-column. In numerical examples, the clamped-clamped, hinged-clamped and hinged-hinged end constraints were considered. The variations of frequency parameters and first buckling load parameters with the non-dimensional system parameters are reported in figures, and typical vibrating mode shapes are presented. Also, the configurations of strongest columns were determined.

요 약

이 논문에서는 일정체적의 정다각형 단면을 갖는 보-기둥의 자유진동 및 좌굴하중을 지배하는 미분방정식을 유도하고 이를 수치해석하였다. 정다각형 단면의 단면깊이 변화식으로는 포물선식과 정현식을 채택하였고, 고정-고정, 회전-고정 및 회전-회전의 단부조건에 대하여 고유진동수 및 좌굴하중을 산출하였다. 수치해석의 결과로 무차원 고유진동수와 무차원변수들 사이의 관계 및 무차원 좌굴하중과 단면비 사이의 관계를 그림에 나타내었다. 또한, 최강기둥의 단면비와 좌굴하중을 산출하였다.

1. Introduction

Since beam-columns are basic structural forms, their statics and dynamics have been studied extensively. Many investigators have been concerned with the mechanical behavior of beam-columns with constant volume past three decades[1].

References[2~10] and their citations include the governing equations and the significant historical literature on this subject. Niordson[2], and Kamat and Simites[3] studied on the optimal shape of beam-column which has the largest first natural frequency. The effects of shear deformation and rotary inertia on optimum beam frequencies had been studied by Kamat and Simites[4].

Keller[5], Tadjbakhsh and Keller[6], and Taylor[7]

*Member, Professor, Wonkwang University
**Graduate Student, Wonkwang University

researched on the shape of strongest columns and its buckling loads. Keller and Niordson[8] studied on the tallest columns. The optimal structural design under multiple eigenvalue constraints had been investigated by Masur[9]. Wilson, et al.[10] conducted the stability experiments of strongest column.

Recent theories predict the optimal shapes for both the largest natural frequencies and highest axial loads of the columns. Although many numerical results were presented in the open literature, the configurations of columns were very limited in the various aspects. For examples, the circular cross-section as shapes of cross-section, the linear taper column as variable depths of cross-section, the hinged-hinged end as end constraints, only the first frequencies, not higher frequencies, in free vibration problems were considered in most previous works. Also, the analysis of the free vibrations and buckling loads problems were not conducted in combination, namely conducted separately.

Therefore, the main purpose of the present paper is to investigate both free vibrations and buckling loads of tapered beam-columns of regular polygon cross-section with constant volume. The differential equation is derived for the free vibration of linearly elastic beam-column. The effect of axial load is included. Also, the differential equation governing the buckled shape of beam-column is derived by using the equation for free vibration.

The governing equations were solved numerically by the Heun's method[12] and determinant search method combined with Regula-Falsi method[12]. The parabolic and sinusoidal tapers were chosen as the tapered beam-column with variable cross-sectional depth. In numerical examples, the clamped-clamped, hinged-clamped and hinged-hinged end constraints were considered. The three lowest natural frequencies and buckling loads are presented as functions of non-dimensional system parameters. Also, the section ratios and buckling load parameters of the strongest columns are reported.

2. Beam-Column with Constant Volume

Shown in Fig. 1(a) depicts a tapered beam-column

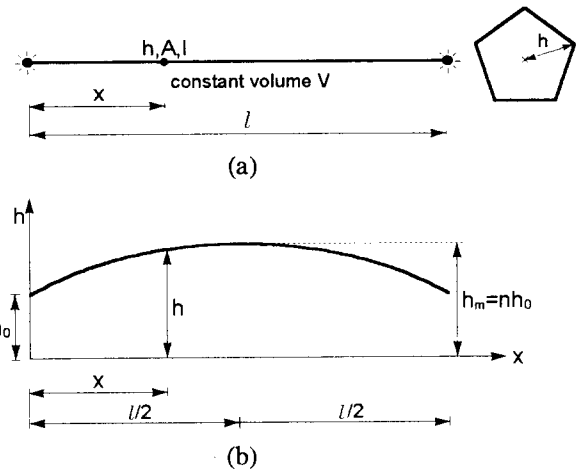

Fig. 1 Beam-column with constant volume and variable cross-sectional depth

with span length l and constant volume V. The beam-column's cross-sectional shape is the regular polygon cross-section and its cross-sectional depth, which is varied with the co-ordinate x, is expressed as h. Therefore, the objective beam-columns have the variable area and variable moment of inertia of cross-section expressed as A and I, respectively. The variation of depth h with x is defined in Fig. 1(b). The depths of both ends($x=0$ and l) and mid-span($x=l/2$) are h_0 and h_m, respectively. Here, a non-dimensional parameter defined as section ratio n is introduced as follows.

$$n=h_m/h_0 \tag{1}$$

The cross-sectional properties A and I of regular polygon cross-section with depth h are, respectively,

$$A=m\sin(\pi/m)\cos(\pi/m)\,h^2 \tag{2}$$

$$I=m\sin(\pi/m)\cos^3(\pi/m)\,[1+\tan^2(\pi/m)/3]\,h^4/4 \tag{3}$$

where m is integer number of sides of polygon. It is clear that A and I with infinite number m, namely circular cross-section, are converged to πh^2 and $\pi h^4/4$, respectively. Also, it is noted that every centroidal axis of regular polygon cross-section is a principal axis and has the same moment of inertia expressed in equation (3).

Now, define the variable cross-sectional depth h shown in Fig. 1(a) and 1(b). In this study, the parabolic and sinusoidal tapers are chosen for the beam-

columns with variable depth h. For the parabolic taper, the function of variable depth h through three points of $(0,\ h)$, $(l/2,\ nh_0)$ and $(l,\ h)$ in rectangular co-ordinates (x,h) is determined as follows.

$$h=h_0[-4\alpha(x/l)^2+4\alpha(x/l)+1],\quad 0\le x\le l \tag{4.1}$$

where,

$$\alpha=n-1 \tag{4.2}$$

The volume V of parabolic taper can now be calculated by using equations (2) and (4.1). The result is

$$V=\int_0^l A\,dx = m\sin(\pi/m)\cos(\pi/m)\,h_0^2 l\beta \tag{5.1}$$

where,

$$\beta=(8n^2+4n+3)/15 \tag{5.2}$$

For sinusoidal taper, the function of variable depth h and volume V are determined:

$$h=h_0[\alpha\sin(\pi x/l)+1],\quad 0\le x\le l \tag{6}$$

in which α is equal to equation (4.2).

$$V=m\sin(\pi/m)\cos(\pi/m)\,h_0^2 l\beta \tag{7.1}$$

where,

$$\beta=\alpha^2/2+4\alpha/\pi+1 \tag{7.2}$$

3. Governing Equations

Figure 2 shows the typical vibrating mode shape of the beam-column subjected to axial load P in which compressive load is positive. Both ends of beam-column are supported by clamped or hinged ends. The beam-column is assumed to be in harmonic motion, or the dynamic displacement $W(x,\ t)$ is proportional to $\sin(\omega t)$ and $w(x)$, where ω is the frequency, t is time and $w(x)$ is the amplitude which is function of x only. The harmonic motion is then

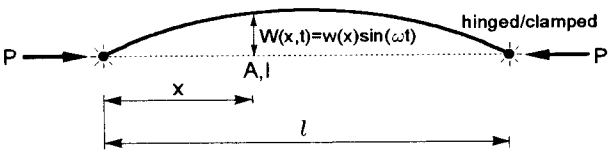

Fig. 2 Typical mode shape of beam-column with an axial load

$$W(x,\ t)=W(x)\sin(\omega t) \tag{8}$$

The partial differential equation governing free vibration of beam-column in which the effect of axial load is included, given in reference[11], is

$$\frac{\partial^2}{\partial x^2}\left[EI\frac{\partial^2 W(x,\ t)}{\partial x^2}\right]+\rho A\frac{\partial^2 W(x,\ t)}{\partial t^2} +P\frac{\partial^2 W(x,\ t)}{\partial x^2}=0 \tag{9}$$

where E is Young's modulus and ρ is mass density. Since A and I are function of x only, the equation (9) is developed as follows.

$$EI\frac{\partial^4 W(x,\ t)}{\partial x^4}+2E\frac{dI}{dx}\frac{\partial^3 W(x,\ t)}{\partial x^3}+\left(E\frac{d^2 I}{dx^2}+P\right) \frac{\partial^2 W(x,\ t)}{\partial x^2}+\rho A\frac{\partial^2 W(x,\ t)}{\partial t^2}=0 \tag{10}$$

Now, substituting each of $\partial^2 W(x,t)/\partial t^2$, $\partial^2 W(x,t)/\partial x^2$, $\partial^3 W(x,t)/\partial x^3$ and $\partial^4 W(x,t)/\partial x^4$ obtained from equation (8) into equation (10) gives the ordinary differential equation governing free vibration of tapered beam-column with axial load P. The result is

$$EI\frac{d^4 w(x)}{dx^4}+2E\frac{dI}{dx}\frac{d^3 w(x)}{dx^3}+\left(E\frac{d^2 I}{dx^2}+P\right) \frac{d^2 w(x)}{dx^2}-\rho A\omega^2 w(x)=0 \tag{11}$$

At hinged and clamped ends, the boundary conditions are

$$w=0 \text{ at hinged end}(x=0 \text{ or } l) \tag{12.1}$$
$$w''=0 \text{ at hinged end}(x=0 \text{ or } l) \tag{12.2}$$
$$w=0 \text{ at clamped end}(x=0 \text{ or } l) \tag{13.1}$$
$$w'=0 \text{ at clamped end } (x=0 \text{ or } l) \tag{13.2}$$

where equations (12.2) and (13.2) assure that the bending moment and rotation are zero, respectively.

To facilitate the numerical studies and to obtain the most general results for this class of problem, the following non-dimensional system variables are introduced:

$$\xi=x/l \tag{14}$$
$$\eta=w/l \tag{15}$$
$$p=Pl^2/(\pi^2 EI_e) \tag{16}$$

$$c_i=\omega_i l^2\sqrt{\rho A_e/(EI_e)},\quad i=1,2,3,\cdots \tag{17}$$

in which ξ and η are normalized by span length l, p is load parameter and c_i is frequency parameter. The subscript i of equation (17) is mode number. Also, A_e and I_e are the area and moment of inertia of cross-section, respectively, of a uniform beam-column with circular cross-section whose volume is V. Such A_e and I_e are determined easily as follows.

$$A_e=V/l \tag{18}$$

$$I_e=(V/2l)^2/\pi \tag{19}$$

When equation (2) and each of dI/dx and d^2I/dx^2 obtained by differentiating equation (3) are substituted into equation (11) and the non-dimensional forms of equations (14)~(17) are used, the result is

$$\frac{d^4\eta}{d\xi^4}=a_1\frac{d^3\eta}{d\xi^3}+(a_2+a_3p)\frac{d^2\eta}{d\xi^2}+a_4c_i^2\eta \tag{20}$$

For parabolic tapers, the coefficients a_1 through a_4 in equation (20) are

$$a_1=32\alpha(2\xi-1)/j \tag{21.1}$$

$$a_2=-32\alpha(28\alpha\xi^2-28\alpha\xi+6\alpha-1)/j^2 \tag{21.2}$$

$$a_3=-\frac{3\pi m\tan(\pi/m)\beta^2}{[3+\tan^2(\pi/m)]}\frac{1}{j^4} \tag{21.3}$$

$$a_4=-\frac{3m\tan(\pi/m)\beta}{\pi[3+\tan^2(\pi/m)]}\frac{1}{j^2} \tag{21.4}$$

where,

$$j=-4\alpha\xi^2+4\alpha\xi+1 \tag{21.5}$$

And for sinusoidal tapers, the coefficients a_1 through a_4 in equation (20) are

$$a_1=-8\pi\alpha\cos(\pi\xi)/j \tag{22.1}$$

$$a_2=4\pi^2\alpha[-3\alpha\cos^2(\pi\xi)/j+\sin(\pi\xi)]/j \tag{22.2}$$

$$a_3=-\frac{3\pi m\tan(\pi/m)\beta^2}{[3+\tan^2(\pi/m)]}\frac{1}{j^4} \tag{22.3}$$

$$a_4=\frac{3m\tan(\pi/m)\beta}{\pi[3+\tan^2(\pi/m)]}\frac{1}{j^2} \tag{22.4}$$

where,

$$j=\alpha\sin(\pi\xi)+1 \tag{22.5}$$

The non-dimensional forms of boundary conditions (12.1)~(13.2) are obtained by using equations (14) and (15):

$$\eta=0 \text{ at hinged end}(\xi=0 \text{ or } 1) \tag{23.1}$$

$$\eta''=0 \text{ at hinged end}(\xi=0 \text{ or } 1) \tag{23.2}$$

$$\eta=0 \text{ at clamped end}(\xi=0 \text{ or } 1) \tag{24.1}$$

$$\eta'=0 \text{ at clamped end}(\xi=0 \text{ or } 1) \tag{24.2}$$

The frequencies decrease as the compressive loads P increase and then, the frequencies vanish when the compressive loads P coincide with the buckling loads. Thus, substituting $c_i=0$ and $p=b_i$ into equation (20) gives the differential equation governing the buckled shapes of beam-column. The result is

$$\frac{d^4\eta}{d\xi^4}=a_1\frac{d^3\eta}{d\xi^3}+(a_2+a_3b_i)\frac{d^2\eta}{d\xi^2} \tag{25}$$

in which b_i is buckling load parameter defined as

$$b_i=B_il^2/(\pi^2EI_e),\quad i=1,2,3,\cdots \tag{26}$$

where B_i is buckling load and i is mode number.

4. Numerical Methods

Based on above analysis, two FORTRAN computer programs were written to calculate frequency parameters c_i and mode shapes $\eta_i=\eta_i(\xi)$, and buckling load parameters b_i for given geometries of beam-columns. The Heun's method[12] was used to integrate the differential equations and then, the determinant search method combined with the Regula-Falsi method[12] was used to determine both eigenvalues of c_i and b_i. For the sake of completeness, the numerical methods were summarized as follows. The first is the free vibration problem.

(1) Specify the beam-column geometry(end constraint, m, n and p) and set of two homogeneous boundary conditions which are either equations (23.1) and (23.2) or (24.1) and (24.2)

(2) Consider fourth order system, equation (20), as two initial value problems whose initial values are the two homogeneous boundary conditions $\xi=0$, as chosen in step (1). Then, assume a trial frequency parameter c_i in which the first trial value is zero.

(3) Using Heun's method, integrate equaton (20) from $\xi=0$ to 1. Perform two separate integrations, one for each of the two boundary conditions.

(4) From the Heun's solution, evaluate at $\xi=1$ the determinant D of coefficient matrix for the boundary conditions of equations (23.1) and (23.2) or (24.1) and (24.2). If $D=0$, then the trial value of c_i is an

eigenvalue. If not, then increment c_i and repeat the above calculations.

(5) In each iteration, note the sign of D. If D changes sign between two consecutive trials, then the eigenvalue lies between these last trial values of c_i.

(6) Use the Regula-Falsi method to compute the advanced trial c_i based on its two previous values.

(7) Terminate the calculations and print the value of c_i and the corresponding mode shape η_i when the convergency criteria are met.

The second is the buckling load problem. Same procedure mentioned above was used for a given beam-column geometry(end constraint, m and n). And it is clear that the eigenvalue in equation (25) is the buckling load parameter b_i. In numerical examples, the lowest three frequency parameters c_i(i=1,2, 3) and only the first buckling load parameters b_1 are calculated.

5. Numerical Examples and Discussions

The first series of numerical studies are shown in Table 1. These studies served to validate the analysis presented herein. Table 1 shows that the numerical results of this study quite agree with the reference values.

Table 1 Comparison of results between references and this study

● Free vibration problem

Geometry*	Data source	c_1	c_2	c_3
$n=1.2$	SAP90	16.19	53.56	114.2
$p=0$	this study	16.19	53.41	112.8
$n=2.0$	SAP90	14.13	48.23	106.2
$p=0$	this study	14.13	47.89	105.4

*$m=3$, parabolic taper, hinged-hinged end

● Buckling load problem

Geometry*	Data source	Ref. value	This study
$n=1$	Ref.[13]	$b_1=1.0$	$b_1=1.0$
$n=2.32$**	Ref.[10]	$B_1=550$ lbs (2447 N)	$B_1=553$ lbs (2460 N)

*Circular cross-section, sinusoidal taper, hinged-hinged end

** $V=9\pi/16$ in^3(2.896×10^{-5} m^3), $l=15.44$ in(0.3922 m), $E=10\times10^6$ psi(6.895×10^{10} Pa)

It is shown in Fig. 3, for which parabolic taper, hinged-hinged end, and $p=0$, that all of the frequency parameters reach a peak as the section ratio n is increased. Further, as the integer numbers m of sides of polygon cross-section increase from $m=3$(triangular cross-section) to $m=4$(rectangular cross-section) to $m=\infty$(circular cross-section), each value of c_i decreases, other parameters remaining constant.

It is shown in Fig. 4, for which $m=4$, sinusoidal

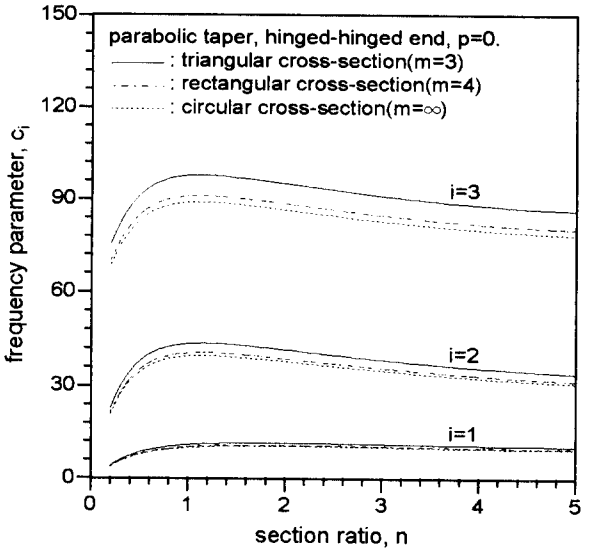

Fig. 3 c_i versus n curves by side number m

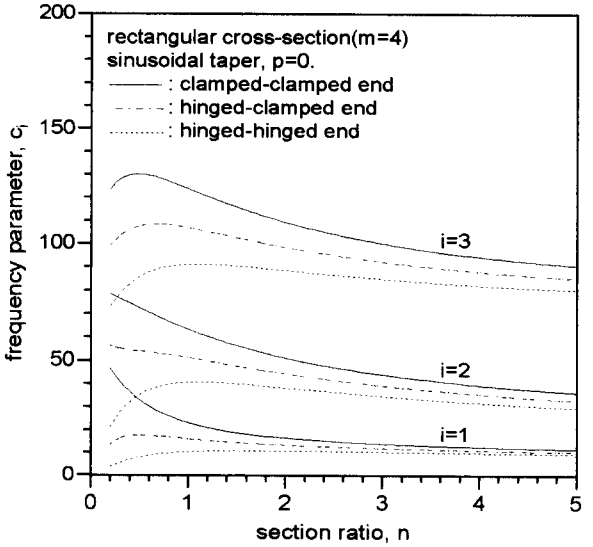

Fig. 4 c_i versus n curves by end constraints

taper, and $p=0$, that several of the frequency parameters reach a peak as the section ratio n is increased. Also, as the end constraints increase from hinged-hinged to hinged-clamped to clamped-clamped, each value of c_i increases, other parameters remaining constant.

It is shown in Fig. 5, for wich $m=\infty$, clamped-clamped end, and $p=0$, that the two c_i versus n curves between parabolic and sinusoidal tapers are compared. Since two curves are very close each other, the effect of tapers on frequencies are negligible, other parameters remaining constant.

It is shown in Fig. 6, for which parabolic taper, hinged-hinged end, and $n=1.25$, that the frequency parameters decrease, as the load parameter is increased. It is clear that p values of horizontal axis met with c_i versus p curves for $i=1$ are the first buckling load parameters for given geometries. After buckling due to the first buckling load, the second and third natural frequencies are meaning-

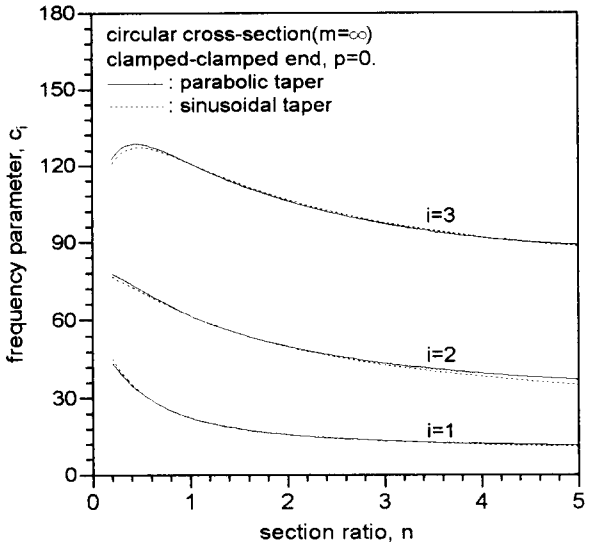

Fig. 5 c_i versus n curves by tapers

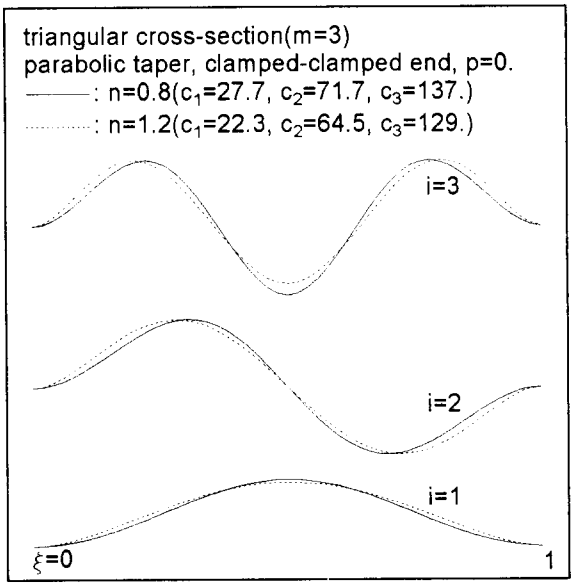

Fig. 7 Example of mode shapes

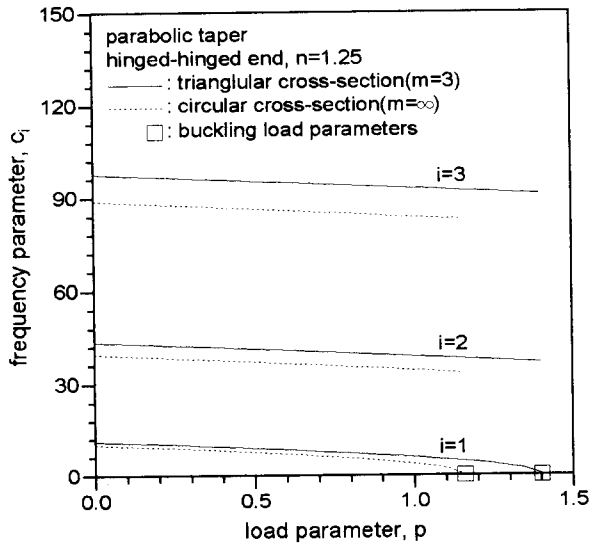

Fig. 6 c_i versus p curves for $m=3$ and circular cross-section

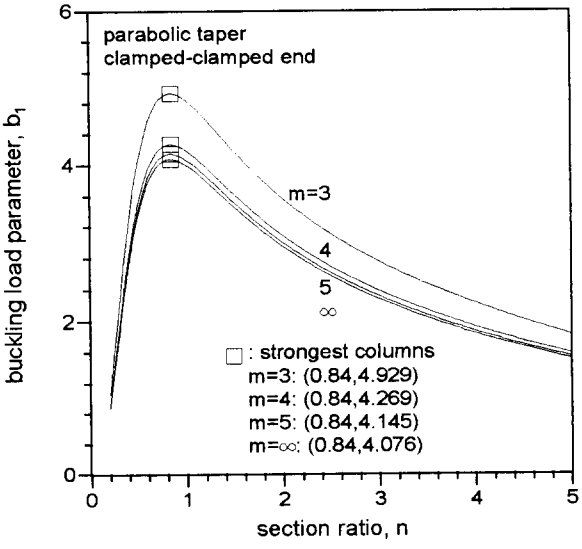

Fig. 8 b_1 versus n curves of parabolic taper for clamped-clamped end

less.

Shown in Fig. 7 are the predicted frequency parameters c_i(i=1,2,3) and their corresponding mode shapes for both n=0.8 and 1.2 for which m=3, parabolic taper, clamped-clamped end, and p=0. It is seen that there are differences between two mode shapes in nodal points and amplitudes.

Shown in Figs. 8, 9 and 10 are the variations of first buckling load parameter b_1 with section ratio n of clamped-clamped, hinged-clamped and hinged-hinged ends, respectively, for parabolic taper. All of buckling load parameters of b_1 reach a peak, as the section ratio n is increased. The peak point of each curve marked □ represents the strongest column which shows the largest buckling load parameter. For example in Fig. 8, the buckling load parameter and section ratio of strongest columns for m=3(triangular cross-section), parabolic taper, and clamped-clamped end are 4.929 and 0.84, respectively, as shown in the legend. It is found that the section

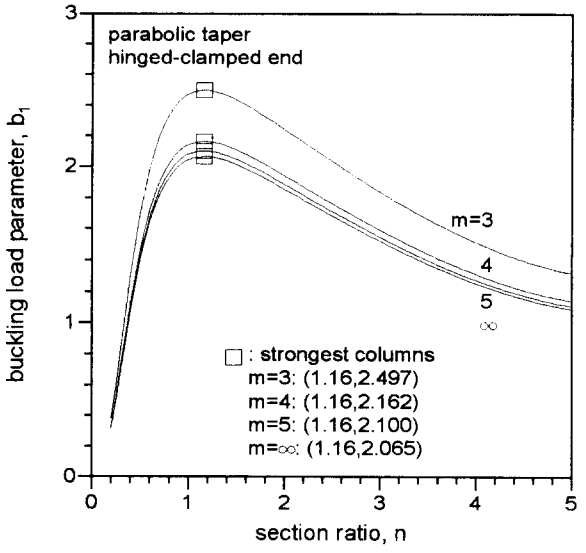

Fig. 9 b_1 versus n curves of parabolic taper for hinged-clamped end

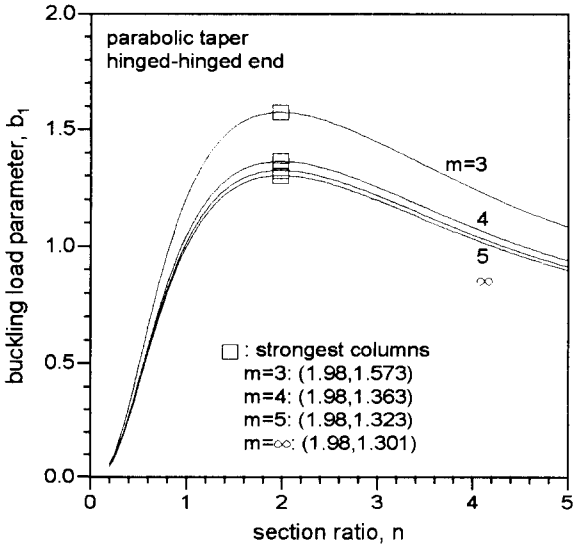

Fig. 10 b_1 versus n curves of parabolic taper for hinged-hinged end

Table 2 Configuration of strongest beam-columns for parabolic taper

End constraint	m	n	b_1
Clamped-Clamped	3	0.84	4.929
	4	0.84	4.269
	5	0.84	4.145
	∞*	0.84	4.076
Hinged-Clamped	3	1.16	2.497
	4	1.16	2.162
	5	1.16	2.100
	∞	1.16	2.065
Hinged-Hinged	3	1.98	1.573
	4	1.98	1.363
	5	1.98	1.323
	∞	1.98	1.301

*∞ : Circular cross-section

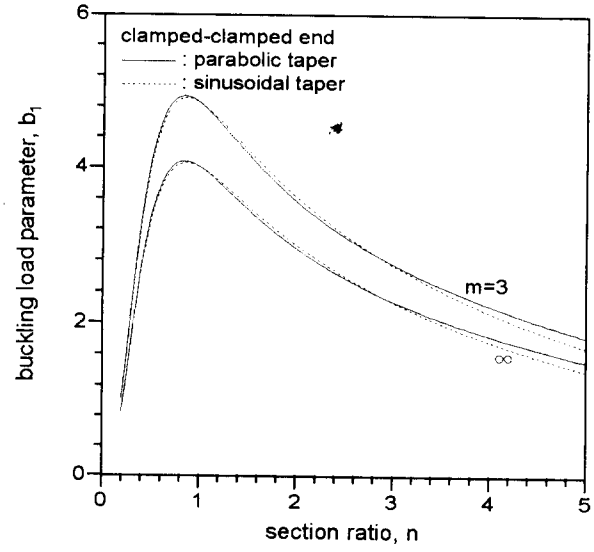

Fig. 11 b_1 versus n curves of clamped-clamped end by tapers

ratios of strongest columns are same regardless of number m of sides of polygon cross-section, taper and end constraint remaining constant. The section ratios and first buckling load parameters of the strongest columns for the parabolic taper are summarized in Table 2.

The effects of taper on first buckling load parameter for clamped-clamped end are presented in Fig. 11. The solid(parabolic taper) and dashed(sinusoidal taper) curves are very close each other so that the taper effect is negligible.

6. Conclusions

The numerical methods developed herein for computing frequencies and buckling loads of beam-columns with constant volume were found to be especially robust and reliable over a wide and practical range of system parameters. Both differential equations governing free vibrations and buckling loads of the beam-columns were derived. The parabolic and sinusoidal tapers with regular polygon cross-sections were chosen as the variable taper. The equations were solved numerically using Heun's method and determinant search method for numerical integrations and calculating the eigenvalues, respectively.

In numerical examples, the clamped-clamped, hinged-clamped and hinged-hinged end constraints were considered. As the numerical results, the variations of frequency parameters with section ratio and load parameter are reported, and typical mode shapes are presented. Also, the variations of first buckling load parameters with section ratios are presented, and the configuration of strongest beam-columns were determined.

References

(1) R. T. Haftka, Z. Grudal and M.P. Kamat, 1990, Elements of Structural Optimization, Kluwer Academic Publisher.

(2) F.I. Niordson, 1965, "On the Optimal Design of a Vibrating Beam," Q.App. Math., Vol. 23, pp. 47~53.

(3) M.P. Kamat and G.J. Simites, 1973, "Optimal Beam Frequencies by the Finite Element Displacement Method," Intl. J. Solids Struct., Vol. 9, pp. 415~429.

(4) M.P. Kamat and G.J. Simites, 1975, "Effect of Shear Deformations and Rotary Inertia on Optimum Beam Frequencies," Intl. J. Num. Meth. Eng., Vol. 9, pp. 51~62.

(5) J.B. Keller, 1960, "The Shape of the Strongest Column," Archiv. Rat. Mech. and Anal., Vol. 5, pp. 275~285.

(6) I. Tadjbakhsh and J.B. Keller, 1962, "Strongest Columns and Isoperimetric Inequalities for Eigenvalues," J. App. Mech., ASME, Vol. 29, pp. 159~164.

(7) J.E. Taylor, 1967, "The Strongest Column-An Energy Approach," J. Appl. Mech., ASME, Vol. 34, pp. 486~487.

(8) J.B. Keller and F.I. Niordson, 1966, "The Tallest Column," J. Math. and Mech., Vol. 16, No. 5, pp. 433~446.

(9) E.F. Masur, 1984, "Optimal Structural Design under Multiple Eigenvalue Constraints," Int. J. Solids Struct. Vol. 20, pp. 211~231.

(10) J.F. Wilson, D.M. Holloway and S.B. Biggers, 1971, "Stability Experiments on the Strongest Columns and Circular Arches," Experimental Mechanics, Vol. 11, pp. 303~308.

(11) R.W. Clough and J. Penzien, 1993, Dynamics of Structures, 2nd Edition, McGraw-Hill.

(12) B. Carnahan, H.A. Luther and J.O. Wilkes, 1969, Applied Numerical Methods, John Wiley & Sons, Inc.

(13) S.P. Timoshenko and J. M. Gere, 1961, Theory of Elastic Stability, McGraw-Hill.